Published in final edited form as:
Cancer Res. 2009 September 1; 69(17): 6941–6950. doi:10.1158/0008-5472.CAN-08-4004.

Inhibitors of deacetylases suppress oncogenic KIT signaling, acetylate HSP90, and induce apoptosis in gastrointestinal stromal tumors

Thomas Mühlenberg[1], **Yixiang Zhang**[2], **Andrew J. Wagner**[2], **Florian Grabellus**[1], **James Bradner**[2], **Georg Taeger**[1], **Hauke Lang**[3], **Takahiro Taguchi**[4], **Martin Schuler**[1], **Jonathan A. Fletcher**[5], and **Sebastian Bauer**[1]

[1] Sarcoma Center, West German Cancer Center, University of Essen, Medical School, Germany

[2] Center for Sarcoma and Bone Oncology, Dana-Farber Cancer Institute, Boston, MA

[3] Department of Surgery, University Hospital Mainz, Germany

[4] Division of Human health and Medical science, Graduate School of Kuroshio Science, Kochi University, Nankoku, Kochi, Japan

[5] Department of Pathology, Brigham and Women's Hospital, Harvard Medical School, Boston, MA

Abstract

GIST are characterized by activating mutations of KIT or PDGFRA and treatment with the tyrosine kinase inhibitor imatinib yields responses in the majority of patients. However, most patients develop secondary resistance which is associated with a dismal prognosis. Histone deacetylase inhibitors (HDACI) have been shown to enhance imatinib activity in imatinib-resistant CML. Against this background we explored whether HDACI might provide an alternative therapeutic strategy to KIT/PDGFRA kinase inhibitors in GIST. Inhibition of cell proliferation by HDACI was seen in KIT-positive but not in KIT-negative GIST cell lines, suggesting that HDACI activity is mainly conferred by targeting oncogenic KIT. KIT activity, expression and activation of downstream pathways were strongly inhibited by several HDACI (SAHA, LBH589, valproic acid, trichostatin A and NaButyrate). SAHA and LBH589 induced apoptosis in KIT-positive GIST, and strong synergism with imatinib was observed at low concentrations of SAHA and LBH589. Mechanistically, treatment with HDACI reduced KIT mRNA transcript levels and led to strong acetylation of HSP90 interfering with its activity as KIT chaperone. These results provide preclinical evidence for a disease-specific effect of HDACI in KIT-positive GIST, which could translate into therapeutic activity.

Keywords

KIT; HDAC; SAHA; gastrointestinal neoplasm; sarcoma; GIST

Introduction

Activating mutations of KIT or Platelet derived growth factor receptor A (PDGFRA) represent the key oncogenic events in gastrointestinal stromal tumor (GIST)(1, 2). The imatinib mesylate (IM) small molecule inhibitor of KIT and PDGFRA yields long-lasting responses in the

Correspondence: Sebastian Bauer, MD, Dept. of Internal Medicine/Cancer Research (West German Cancer Center), Hufelandstr. 55, 45122 Essen, Germany, sebastian.bauer@uni-due.de.

majority of patients, with a median survival of almost 5 years(3). However, 20% of patients have primary resistance to IM, and most responding patients eventually develop secondary resistance and progress. Second line therapy with sunitinib yields 7% responses, but patients progress after a median of 6 months with a dismal outcome at time of progression. Therefore, alternative treatment strategies are urgently needed (4).

Secondary mutations within the split kinase domain (exon 13 and 17) of KIT account for acquired IM-resistance in most patients(5)(6). While mutations within the ATP-binding pocket (exon 13, exon 14) are generally sensitive to novel direct KIT-inhibitors such as sunitinib and nilotinib, mutations within the activation loop (exon 17) are often cross resistant to these newer-generation KIT inhibitors(7, 8). Overall, sensitivity to KIT kinase-inhibitors varies considerably depending on the type of secondary mutation. Therefore individual KIT kinase-inhibitor drugs are not likely to inhibit the myriad KIT drug resistance mutations that can be demonstrated, even within the same patient(6). To avoid the pharmacological challenge of genomic heterogeneity, novel therapeutic strategies include inhibition of heat shock protein 90 which has been shown to inhibit oncogenic KIT, irrespective of the underlying secondary mutation(9).

Histone deacetylase inhibitors (HDACIs) represent a promising novel class of anti-cancer agents, several of which are currently undergoing clinical trials in malignant diseases. Acetylation of lysine residues of core histone proteins leads to relaxed chromatin structure and enables transcription(10). HDACI exhibit an apparent selectivity for tumor repressing or cell cycle inhibitory genes (e.g. *gelsolin*, *CDKN1A*/p21^{WAF1} or *CDKN2A*/p16)(11). In addition, a plethora of non-histone proteins that play a key role in oncogenesis and cancer progression are targets of acetylation and deacetylation (e.g. p53, HSP90)(12), and HDACI may exert their activity through these proteins as well(13).

Suberoyl hydroxamic acid (SAHA) is the first HDACI that was approved by the FDA, and is now included in the treatment of recurrent and advanced cutaneous T-cell lymphoma (CTCL) (14). Notably, SAHA has been shown to inhibit IM-resistant BCR/ABL and induce apoptosis in BCR/ABL-positive leukaemia cell lines(15).

Against this background we sought to evaluate the therapeutic relevance of HDACI in gastrointestinal stromal tumors *in vitro*.

Materials and Methods

Cell lines

GIST-T1 was established from a human, untreated, metastatic GIST containing a 57bp deletion in exon 11(16). GIST882, as previously described, was established from an untreated human GIST with an homozygous missense mutation in KIT exon 13, encoding a K642E mutant KIT oncoprotein(17). GIST48 was established from a GIST that had progressed, after initial clinical response, during IM therapy. GIST48 has a primary, homozygous exon 11 missense mutation (V560D) and a heterozygous secondary exon 17 (kinase activation loop) mutation (D820A). GIST48B is a subline of GIST48 which, despite retaining the activating KIT mutation in all cells, expresses KIT transcript (data not shown) and protein at essentially undetectable levels. GIST62 was also derived from a KIT-positive GIST with a KIT exon 11 in-frame mutation that has subsequently lost KIT expression(9). GIST522 was established from an IM-resistant, progressing GIST and contains a primary heterozygous KIT exon 11 mutation (delEVQWK554–558). However, the KIT oncoprotein has been transcriptionally silenced. The KIT-negative cell lines serve as a negative control for evaluation of KIT inhibitors, but in a GIST cell context.

Leiomyosarcoma cell lines LMS03 and SK-LMS-1 were established from high-grade leiomyosarcomas, LPS141 from a dedifferentiated liposarcoma, and RMS176 from an embryonal rhabdomyosarcoma.

Reagents and Antibodies

Imatinib mesylate and LBH589 were kindly provided by Novartis Pharma (Basel, Switzerland). SAHA was from Alexis (Lausen, Switzerland), TSA, and VPA were purchased from Calbiochem (Merck, Darmstadt, Germany). A rabbit polyclonal antibody to KIT was from DAKO (Carpinteria, CA). Polyclonal rabbit antibodies to phospho-KIT Y703, and PARP were from Zymed Laboratories (South San Francisco, CA). Polyclonal rabbit antibodies to total p42/44 mitogen-activated protein kinase (MAPK), phospho-p44/42 MAPK T202/Y204, phospho-AKT S473, total AKT, phospho-PKCtheta (Thr538), cleaved caspase 3, phospho-KIT Y719, acetylated-lysine and Histone H3 were from Cell Signaling (Beverly, MA). Polyclonal goat antibody for total PKCtheta, HSP70 monoclonal mouse antibody and polyclonal rabbit antibody against HDAC6 were from Santa Cruz Biotechnology (Santa Cruz, CA). p21 and s-Actin Antibodies were purchased from Sigma (St. Louis, MO). Acetylated Histone H3 antibody was from Upstate Biotechnology (Lake Placid, NY). A HSP90 antibody was from Stressgen (Ann Arbor, MI).

In vitro assays

Viability studies were carried out using the CellTiter-Glo luminescent assay (Promega, Madison, WI), in which the luciferase catalyzed luciferin/ATP reaction provides an indicator of cell number (18). For these studies, the cell lines were plated at 15 to 30,000 cells per well in a 96-well flat-bottomed plate (Falcon, Lincoln, NJ), cultured in serum-containing media for 1 to 2 days, and then incubated for 72 hours with HDAC-, or KIT-inhibitors or DMSO-only solvent control. The CellTiter-Glo assay luminescence was measured with a Genion Luminometer (Tecan, Crailsheim, Germany) and the data were normalized to the DMSO-only control group. All experimental points were measured in quadruplicate wells for each plate and were replicated in at least two plates.

Apoptosis studies were done by measuring caspase-3 and caspase-7 activation with the Caspase-Glo 3/7 Assay Kit (Promega). This assay uses a proluminescent substrate containing the DEVD sequence recognized and activated by caspase-3 and caspase-7 (19, 20) and the luminescence signal is proportional to net caspase-3 and caspase-7 activation(21). The experimental conditions were all as described above for the CellTiter-Glo studies except treatment duration of 24 and 48 hours.

Western blotting and immunoprecipitation

Protein lysates were prepared from cell line monolayers according to standard protocols(22). Protein concentrations were determined with the Bio-Rad Protein Assay (Bio-Rad Laboratories, Hercules, CA). Electrophoresis and immunoblotting were carried out as previously described (23). Changes in protein expression and phosphorylation as visualized by chemiluminescence were captured and quantified using a FUJI LAS3000 system with Science Lab 2001 ImageGauge 4.0 software (Fujifilm Medial Systems, Stamford CT, USA).

Immunoprecipitations were performed with Sepharose protein G beads (Zymed Laboratories) from 400–600 μg of total protein as described previously(9).

Cell cycle analysis

Cells were plated in six-well plates, grown until 80% confluence, and then treated for 48 hours with DMSO, SAHA (2 μM), or IM (500 nM) and a combination of both drugs. Cells were then

trypsinized and stained with DNA prep containing propidium iodide (PI) (Beckman Dickonson, Heidelberg, Germany) followed immediately by flow cytometric analysis (BeckmanCoulter FC500 Flow Cytometer). Modfit LT software 3.1 (Verity Software House, Topsham, ME) was used for data analysis.

Cell viability assessment by Annexin V Staining

After drug treatments for 48 hours, cells were resuspended in 500 μl of the staining buffer and annexin V FITC (525 nm) and 7-AAD (675 nm) were added. After incubation at room temperature for 15 min, annexin V-positive cells were estimated by flow cytometry. 10000 events of each sample were acquired on a BeckmanCoulter FC500 Flow Cytometer. Doublet discrimination was done with FL2 vs. FL2 peak histogram.

Quantitative Real Time Reverse Transcriptase-PCR

Cells were plated in 12-well plates, grown until 80% confluence, and then treated with drug-containing media. Cells were then collected with RNAprotect Cell reagent (Quiagen, Hilden, Germany) and processed with RNeasy Mini Kit (Quiagen) according to the manufacturer's protocol, for RNA isolation. cDNA was transcribed by Reverse Transcriptase-PCR using random primers and *KIT*-cDNA was amplified and measured using TaqMan gene expression assays (Applied Biosystems, Softer City, CA) and Real Time PCR system LightCycler 480 (Roche, Grenzach-Wyhlen, Germany). Beta Actin cDNA, (also measured using Taqman gene expression assay (AB)) served as reference gene for relative quantification.

Results

HDACI exhibit anti-proliferative effects in KIT-positive cell lines

We first evaluated the antiproliferative effects of SAHA in GIST cell lines by treating cells for 72h with increasing concentrations of SAHA (10 nM to 10 μM), as well as with IM 500 nM alone and in combination with SAHA 2.5 μM.

SAHA treatment resulted in strong antiproliferative effects in IM-sensitive GIST882 and GIST-T1 (IC50=3.5 μM and 1.7 μM, respectively) and IM-resistant GIST48 (IC50=3.2 μM) but not in KIT-negative GIST48B, GIST62 and GIST522 (IC50 >10 μM; Figure 1a). Combination of SAHA with IM (500 nM) yielded slightly additive effects (Figure 1b) in KIT-positive cell lines but not in KIT-negative GIST48B. For combination studies, a clinically relevant dose of IM which substantially inhibits KIT signaling in IM-sensitive but not IM-resistant GIST was used.

Sarcomas other than GIST are less sensitive to HDACI

To study GIST-independent effects of HDACI we then compared SAHA antiproliferative effects in GIST to those induced in several other soft tissue sarcoma cell lines (Figure 1c). IC50s ranged from 2.8 μM in the rhabdomyosarcoma cell line RMS176 to 5 μM in the leiomyosarcoma cell line SK-LMS-1 but were not reached in LMS03 and LPS141 (inhibition of 35% and 24% at 10 μM).

HDAC-inhibition induces apoptosis in KIT-positive but not in KIT-negative GIST, which is enhanced by imatinib

To study induction of apoptosis by HDACI, cells were plated in 96-well plates and treated with SAHA at concentrations ranging from 1 μM to 5 μM singly or in combination with IM 500 nM for 24 and 48h and then analysed for caspase 3/7 activation. In GIST882, SAHA alone resulted in a maximum of 5.9-fold induction, compared with control, and IM treatment showed

a 3.7-fold induction. Notably, combination of SAHA 5 μM and IM 500 nM after 48h resulted in a 15-fold induction of activated caspase 3/7, compared to vehicle control.

In IM-resistant GIST48, additive effects of combination treatment with IM 500 nM and SAHA 5 μM (13-fold) after 24h were less pronounced than those seen in GIST882, compared with IM and SAHA alone (5-fold and 11-fold increase, respectively (Figure 2a)). Notably, combinations of imatinib with lower doses of SAHA (1 μM and 2 μM) resulted in synergistic pro-apoptotic effects.

We further evaluated apoptosis in cell lysates from GIST cells that were treated with SAHA for 18h. SAHA at concentrations ≥ 2 μM resulted in dose-dependent cleavage of caspase 3 and the caspase substrate PARP (86kDa-fragment) when measured by western blot in GIST882, GIST-T1 and GIST48 (Figure 2b). Combination of IM 500 nM and SAHA at 2 μM induced caspase 3 cleavage comparable to that induced by 10 μM SAHA alone. GIST48 caspase cleavage was demonstrable at 2 μM SAHA, with a two-fold induction at 5 μM and a synergistic effect when 2 μM of SAHA were combined with IM, with the combination exceeding cleavage levels seen with 10 μM of SAHA alone. In contrast, no induction of apoptosis markers was seen in KIT-negative GIST48B (Figure 2b). Representative apoptosis studies were also performed with LBH589 in GIST882 which at 500 nM showed a 7.4-fold induction of caspase-3 cleavage and 7.8-fold induction of PARP cleavage. Again, synergistic induction was demonstrated when LBH589 was combined with IM (Supplemental Figure 1).

We further performed apoptosis assessment by Annexin V/7-AAD staining in GIST882. 48 hours of treatment with IM (500 nM), SAHA (2 μM) and LBH589 (25 nM) resulted in moderate induction of early apoptosis (15%, 7% and 20%, respectively) when given singly (Supplemental Figure 2). In contrast, combinations of IM with SAHA or LBH589 at the same dose levels showed a synergistic proapoptotic effect resulting in early apoptosis in 38% (IM plus SAHA) and 49% (IM plus LBH589) of GIST 882 cells.

For cell cycle analyses GIST882 cells were treated for 48 hours with DMSO, IM (500 nM), SAHA (2 μM) and LBH589 (25 nM) which resulted a low sub-G1 fraction (1%, 13%, 2% and 5%) while combinations of both SAHA and LBH589 resulted in additive increase of subG1 cells (29 and 36%). With regard to effects of inhibitors on cell cycle distribution, IM showed a strong reduction of the S-phase while other inhibitors did not. No other substantial changes were observed (Supplemental Figure 3).

HDACI inhibit KIT- and KIT-dependent signaling pathways

To elucidate the mechanism of HDACI-induced sensitization to apoptosis, we investigated the effects of HDAC-inhibitors on KIT and KIT-depending signaling pathways. To avoid confounding effects of cell apoptosis and general disruption of the cellular architecture, an early time point (18 hours) was chosen as used in similar experiments by other groups(13). In GIST882, GIST-T1 and GIST48, SAHA treatment resulted in marked inhibition of KIT-phosphorylation (GIST882 and GIST-T1: IC50 1.7 μM, near total inhibition at 5 μM; GIST48: IC50 3 μM, 81% inhibition at 5 μM), which was paralleled by substantial inhibition of phospho-AKT and phospho-MAPK (Figure 3a), and by decreased total KIT expression (70% and 80% decrease at 5 μM in GIST-T1, GIST882 and GIST48) involving equally the mature (160kDa) and immature (145kDa) forms of KIT. LBH589 showed a similar, dose-dependent effect on KIT and KIT-depending signalling at 20-fold lower concentrations (IC50 for inhibition of p-KIT = 105 nM; total KIT = 190 nM, pAKT = 30 nM; pMAPK = 190 nM (Supplemental Figure 1)).

In KIT-negative GIST48B, no detectable levels of phosphorylated KIT and minimal levels of total KIT were found. SAHA treatment caused a minor decrease in phospho-MAPK starting at 2 μM, with partial inhibition at 5 μM (Figure 3a).

Time course studies on GIST882 cells were performed to determine the onset of KIT inhibition in correlation to histone acetylation. Cells were treated for 30 minutes to 24 hours with 5 μM SAHA (Figure 3b). Immunoblots for KIT and for KIT-depending signaling pathways revealed near total inhibition of phospho-KIT, total KIT, pAKT and pMAPK after 9 hours. Caspase cleavage was demonstrated at 12 hours and peaked at 24 hours. Induction of cell cycle protein p21 started at 3 hours of treatment. Notably, acetylation of core histone protein H3 was observed at the 12 hour time point and peaked at 24 hours.

Effects of a HDACI panel on GIST viability

We then evaluated other HDACI, including Trichostatin A (TSA), valproic acid (VPA), sodium butyrate(NaB) and LBH589 which showed IC50s between high nM (LBH589, TSA) to low mM (NaB, VPA) concentrations, with only minor differences seen between IM-sensitive and IM-resistant cells (Figure 4a and b). Additive antiproliferative effects were seen with all HDACI and IM in GIST48 (Figure 4c). Notably, LBH589, a third-generation pan-deacetylase inhibitor, was 22 and 39 times more potent than SAHA against GIST48 and GIST882 respectively (Figure 4a and b).

Effects of HDACI on histone H3 acetylation

The lowest SAHA concentrations inducing histone H3 acetylation were 1 μM in GIST882, 0.5 μM in GIST-T1, GIST48 and GIST48B (Figure 2b), and for LBH589 were 10 nM in GIST882 and GIST48 (Supplemental Figure 1). Notably, minor induction of total H3 was observed. Of note, combination treatment of HDACI (SAHA and LBH589) and IM resulted in synergistic induction of histone acetylation (Figure 2b, Supplemental Figure 1). While LBH589 at 100 nM resulted in 5.5-fold induction of histone acetylation, the combination with IM resulted in 15-fold induction (Supplemental Figure 1).

GIST histone H3 acetylation and KIT-inhibition differ after treatment with various HDACI

The effects of several HDACI were compared on pKIT, pAKT, acetylated and total histone H3 (Figure 4d) after 18h treatment, using two concentrations for each HDACI, around the IC50s established previously in the GIST882 proliferation studies. Inhibition of pKIT was by far strongest for cells treated with SAHA, while other HDACI showed only minor pKIT inhibition. Notably, KIT-inhibition differed between SAHA 2 μM, TSA 300 nM, VPA 3 mM and NaB at 1 mM despite comparable levels of histone acetylation. Interestingly, moderate inhibition of pKIT was accompanied by complete inhibition of pAKT following treatments with NaB and VPA (Figure 4d).

SAHA decreases KIT-RNA in a time and dose dependent manner

To evaluate the effect of HDAC inhibition on *KIT* transcript levels, real time PCR was performed following treatment of GIST882 with SAHA 2 μM and 5 μM for 4h, 8h, and 12h (Figure 5a). *KIT* transcripts decreased in a time and dose-dependent manner in GIST882, with a decrease of 70% using SAHA 2 μM and 84% using SAHA 5 μM, after 12h of treatment (Figure 5a). By contrast, GIST882 treatment with IM at this time showed no reduction compared to DMSO. We then compared SAHA effects at 12 hours with LBH589 and 17-AAG and found a similarly strong decrease of *KIT* mRNA levels following LBH589, but not after 17-AAG, in GIST 882 and GIST48 (Figure 5b). The KIT-negative liposarcoma cell line LPS141 showed 10^{-4} times lower levels of *KIT* mRNA levels compared with the untreated GIST cell lines (Figure 5b).

Given the important role of PKCtheta in the regulation of KIT expression(24) we also investigated the effects of HDACI on PKCtheta expression and phosphorylation (Supplemental Figure 4). Notably, SAHA and LBH589 were shown to reduce expression of both total and phosphorylated PKCtheta by 20–40%.

To evaluate the half-life of KIT following block of translation we treated GIST882 with 100 μM cycloheximide (CHX) in a time-course experiment and found >80% reduction of total KIT after 3 hours and near-total loss after 6 hours (Figure 5c).

HDACI inhibit KIT through acetylation of HSP90

In order to investigate possible non-histone related KIT-inhibitory mechanisms we treated GIST882 with SAHA 5 μM for 12 hours, then performed immunoprecipitation for HSP90, and counterstained with anti-acetyl lysine and HDAC6. Substantial increase of HSP90 acetylation was demonstrated following SAHA treatment (Figure 6) while HDAC6 dissociated from HSP90 (Figure 6a). These findings were confirmed by immunoprecipitation of HDAC6, where we demonstrated commensurate dissociation of HSP90 (Figure 6b). KIT immunoprecipitations revealed increased binding of HSP70 to KIT while HSP90 was found to slightly dissociate when normalized to relative levels of KIT (Figure 6c).

Discussion

Identification of KIT as a crucial oncogenic regulator pathway has revolutionized the treatment of GIST(25). The KIT-inhibitor imatinib has tripled the median survival of patients with metastatic GIST and many patients live 5 years or longer with the disease. However, most patients inevitably develop resistance. Resistance is mostly conferred by secondary mutations within the split kinase domain of KIT(6, 27, 28). While resistance mutations within the ATP-binding domain (T670I, V654A) can successfully be targeted by alternative KIT-inhibitors such as sunitinib, mutations within the activation loop are an ongoing pharmacologic challenge (29–31). In addition, more than 9 different resistance mutations have already been described and different mutations may even occur within the same patient(6, 32, 33). Direct, ATP-competitive inhibitors are therefore unlikely to sufficiently inhibit all possible KIT mutations.

Alternative strategies aim to inhibit the oncogenic signal of KIT regardless of existing secondary mutations. Among those are inhibition of KIT-dependent signaling pathways (e.g. PI3K, AKT or mTOR(34, 35)) or indirect inhibition of KIT using HSP90 inhibitors(9, 36, 37) which are already being tested clinically.

The post-translational modification of histones, e.g. through acetylation and deacetylation of lysine-tails, has been shown to be an important mechanism of transcriptional regulation(38). Interestingly, many genes upregulated by HATs are important for differentiation, cell cycle control and apoptosis(39). Aberrant acetylation, either through overexpression of HDAC or HAT dysfunction is commonly found in epithelial and hematological cancers (40–42). In this context HDAC inhibitors exhibit an apparent selectivity for activating transcription of tumor-suppressing genes(39).

Recently, several groups have highlighted the potential therapeutic relevance of HDAC inhibitors in IM-resistant chronic myelogenous leukemia cells. HDACI destabilized the BCR-ABL oncoprotein even in the presence of the highly IM-resistant T315I gatekeeper mutation (13, 43, 44). Given the similarities of the oncogenic tyrosine-kinase-mechanisms between CML and GIST we therefore investigated the potential therapeutic value of HDACI in GIST.

The data reported herein are the first to show strong antiproliferative and proapoptotic effects in both IM-sensitive and IM-resistant GIST by inhibitors of histone deacetylases. We show

that these effects are conferred by inactivation of the KIT-oncogenic signaling cascade. The inactivation mechanisms include both inhibition of *KIT* transcript expression and also degradation of KIT oncoproteins via suppression of deacetylation of the KIT chaperone HSP90.

KIT-positive GIST lines were sensitive to HDACI (IC50 1.7–3.5 μM), while KIT-negative GIST lines were unresponsive (Figure 1). These findings compare well with data from other SAHA sensitive cancer cell lines, for which IC50s (SAHA) in the low micromolar dose range were described(15, 43, 45). These dose levels are considered to be therapeutically achievable. Antiproliferative effects of HDACI were lower in non-GIST sarcomas, with only 10–20% inhibition after treating leiomyosarcoma (LMS03) and liposarcoma (LPS141) cell lines with 10 μM SAHA indicating that GISTs are uniquely susceptible to HDACI.

In KIT-positive GISTs, HDACI treatment induced dose-dependent inhibition of KIT phosphorylation, paralleled by AKT inhibition (Figure 3a). In GIST882, inhibition of AKT-phosphorylation was even more pronounced with all HDACI used than inhibition of KIT phosphorylation (Figure 3, 4 Supplemental Figure 1), suggesting that HDACI may have inhibitory effects on the PI3K-AKT pathway independent of KIT inhibition. Interestingly, in studies with different HDACI, the effects on histone acetylation did not strictly correlate with KIT inhibition, suggesting that KIT-inhibitory effects are partly histone independent and perhaps dependent on certain HDAC subtypes. While TSA, SAHA and LBH589 are pan HDACI, VPA and NaB only inhibit class I HDACs.

Our studies suggest that HDACI have several mechanisms contributing to KIT inhibition: Histone acetylation may cause reduced KIT transcription, most likely by affecting expression of *KIT* transcriptional repressors. HDACI might also regulate oncoprotein function, e.g. by modifying KIT acetylation, and may influence KIT oncogenic signaling through effects on non-histone HDACI targets.

Direct, ATP-competitive inhibitors of KIT, such as IM, are known to have KIT-inhibitory effects within several minutes of treatment (data not shown). Time course-studies with HDACI (Figure 3b) showed onset of KIT inhibition after 3 and 6 hours of treatment, with a maximum effect between 12 and 18 hours. Only subtle histone acetylation was seen at the early time points (3–6h) and the maximal acetylation level was seen only at the last time point (24h). These findings suggest the possibility of HDACI-mediated indirect inhibition of KIT rather than a direct, biochemical inhibition as seen with IM. Notably, signalling studies demonstrated both inhibition of KIT phosphorylation and decreased KIT expression. While direct KIT inhibitors such as IM and sunitinib do not decrease total KIT expression, we have previously shown that HSP90 inhibitors strongly decrease KIT expression levels(9).

HSP90 is known to be subject to several posttranslational modifications that affect its function. Hyperacetylation of HSP90, especially acetylation of the amino acid K294, decreases the affinity for most clients and certain cochaperones(46, 47). Inhibition of HDAC6, a class II HDAC, has recently been shown to disrupt the chaperone function of HSP90 resulting in degradation of HSP90 clients, such as BCR-ABL(12, 13). This appears to be caused by lower affinity for ATP(43). As the assembly of the functional HSP90 chaperone complex requires ATP, HDACI effects on HSP90 can be explained in part by the inhibition of its complex formation. In line with this model we here show that HDACI treatment of GIST cells causes dissociation of HDAC6 from HSP90 resulting in hyperacetylation of HSP90 and a consequent loss of KIT (Figure 6).

Treatment of GIST48B and GIST62 with SAHA resulted in substantial inhibition of pMAPK (GIST48B and GIST62) and pAKT (GIST62) despite the lack of measurable KIT activation

(Figure 3a, data not shown). These findings indicate that apart from HDACI effects on KIT, other signaling pathways might be affected.

Of note, *KIT* transcript levels were found to be downregulated in a time- and dose-dependent fashion, with maximal effects seen after 12 hours of SAHA treatment (Figure 3b). Since HDACI are thought to enable rather than suppress transcription, these effects can be explained by induction of a gene responsible for *KIT* transcriptional repression. The loss of KIT expression seen after 12 hours of treatment with HDACI could be explained both by transcriptional repression and HSP90 inhibition. However, the extent of KIT inhibition due to a transcriptional block at this time point would mainly depend on the half-life of mature KIT in GIST cells. We therefore treated GIST882 with cycloheximide and demonstrated that the KIT half-life, in GIST, is less than 3 hours (Figure 5c). In contrast, the HSP90 chaperone (>24h) or the KIT regulator PKCtheta (>12h) exhibited a more than four times longer half life following cycloheximide treatment (Figure 5c). Ou et al. recently reported that PKCtheta is a major regulator of KIT transcription(24). Notably, HDACI caused partial inhibition of PKCtheta, and PKCtheta inhibition may therefore contribute to the inhibition of KIT expression in GIST.

Mechanisms of resistance to direct KIT-inhibitors largely depend on secondary mutations within the KIT ATP binding pocket or activation loop. Our studies suggest that HDACI-mediated inhibition of KIT oncoproteins is independent of the KIT mutation location, with equal relevance for GISTs with imatinib-sensitive or imatinib-resistant KIT mutations. Hence, HDACI might overcome resistance to both ATP binding pocket and activation loop imatinib-resistance mutations, providing a new strategy to inhibit KIT.

Similar to studies evaluating combinations of IM and HDACI in CML, we found no evidence for antagonistic effects and we identified additive proapoptotic effects in GIST882 and GIST48 (15, 43, 48). Notably, we observed synergistic effects of HDACI and IM on histone acetylation in the KIT-positive GIST lines (Figure 3a) but not in the KIT-negative GIST48B.

We observed induction of p21 by SAHA in all GIST cell lines (Figure 2b), including KIT-negative GIST48B and GIST62 (Figure 2b, data not shown), and this might result directly from histone acetylation (49). However, in the KIT-negative GIST48B and GIST62, p21 induction did not cause marked cell cycle arrest, nor induction of apoptosis (Figure 2B, Supplemental Figures 3, 4; data not shown). These findings suggest that inhibition of oncogenic KIT is the most consequential mechanism of HDACI action in GIST.

Taken together, our data show that HDACI have disease specific effects in GIST by inhibiting the crucial KIT oncogenic pathway. We consistently found additive effects of HDACI and IM in IM-sensitive GIST, regardless of the HDACI used. LBH589 exhibits the highest potency of all HDACI tested even though biological effects of SAHA and LBH589 are similar. Possible mechanisms of action for HDACI in GIST include acetylation of HSP90 with consequent destabilization of KIT, but effects on KIT transcriptional activity may also play a partial role. Given the antiproliferative and proapoptotic effects of HDACI at doses that can be achieved therapeutically, our data provide a strong rationale for the clinical evaluation of HDACI/DACI in GIST.

Supplementary Material

Refer to Web version on PubMed Central for supplementary material.

Acknowledgments

Grant Support: Anonymous Donor, Max-Eder Fellowship from the Dr. Mildred Scheel Stiftung für Krebsforschung (S. Bauer), Life-raft Group Research Initiative (S. Bauer)

Reference List

1. Hirota S, Nishida T, Isozaki K, et al. Gain-of-function mutation at the extracellular domain of KIT in gastrointestinal stromal tumours. J Pathol 2001;193:505–10. [PubMed: 11276010]
2. Heinrich MC, Corless CL, Duensing A, et al. PDGFRA activating mutations in gastrointestinal stromal tumors. Science 2003;299:708–10. [PubMed: 12522257]
3. Blanke CD, Demetri GD, Von Mehren M, et al. Long-term results from a randomized phase II trial of standard- versus higher-dose imatinib mesylate for patients with unresectable or metastatic gastrointestinal stromal tumors expressing KIT. J Clin Oncol 2008;26:620–5. [PubMed: 18235121]
4. Demetri GD, van Oosterom AT, Garrett CR, et al. Efficacy and safety of sunitinib in patients with advanced gastrointestinal stromal tumour after failure of imatinib: a randomised controlled trial. Lancet 2006;368:1329–38. [PubMed: 17046465]
5. Heinrich MC, Corless CL, Blanke CD, et al. Molecular Correlates of Imatinib Resistance in Gastrointestinal Stromal Tumors. J Clin Oncol. 2006
6. Wardelmann E, Thomas N, Merkelbach-Bruse S, et al. Acquired resistance to imatinib in gastrointestinal stromal tumours caused by multiple KIT mutations. Lancet Oncol 2005;6:249–51. [PubMed: 15811621]
7. Prenen H, Cools J, Mentens N, et al. Efficacy of the kinase inhibitor SU11248 against gastrointestinal stromal tumor mutants refractory to imatinib mesylate. Clin Cancer Res 2006;12:2622–7. [PubMed: 16638875]
8. Heinrich MC, Corless C, Liegl B, et al. Mechanisms of sunitinib malate (SU) resistance in gastrointestinal stromal tumors (GISTs). Proc Am Soc Clin Oncol 2007;25:10006.
9. Bauer S, Yu LK, Demetri GD, Fletcher JA. Heat shock protein 90 inhibition in imatinib-resistant gastrointestinal stromal tumor. Cancer Res 2006;66:9153–61. [PubMed: 16982758]
10. Marks P, Rifkind RA, Richon VM, Breslow R, Miller T, Kelly WK. Histone deacetylases and cancer: causes and therapies. Nat Rev Cancer 2001;1:194–202. [PubMed: 11902574]
11. Johnstone RW. Histone-deacetylase inhibitors: novel drugs for the treatment of cancer. Nat Rev Drug Discov 2002;1:287–99. [PubMed: 12120280]
12. Kovacs JJ, Murphy PJ, Gaillard S, et al. HDAC6 regulates Hsp90 acetylation and chaperone-dependent activation of glucocorticoid receptor. Mol Cell 2005;18:601–7. [PubMed: 15916966]
13. Bali P, Pranpat M, Bradner J, et al. Inhibition of histone deacetylase 6 acetylates and disrupts the chaperone function of heat shock protein 90: a novel basis for antileukemia activity of histone deacetylase inhibitors. J Biol Chem 2005;280:26729–34. [PubMed: 15937340]
14. Grant S, Easley C, Kirkpatrick P. Vorinostat. Nature Reviews Drug Discovery 2007;6:21–2.
15. Yu C, Rahmani M, Almenara J, et al. Histone deacetylase inhibitors promote STI571-mediated apoptosis in STI571-sensitive and -resistant Bcr/Abl+ human myeloid leukemia cells. Cancer Res 2003;63:2118–26. [PubMed: 12727828]
16. Nakatani H, Kobayashi M, Jin T, et al. STI571 (Glivec) inhibits the interaction between c-KIT and heat shock protein 90 of the gastrointestinal stromal tumor cell line, GIST-T1. Cancer Sci 2005;96:116–9. [PubMed: 15723656]
17. Tuveson DA, Willis NA, Jacks T, et al. STI571 inactivation of the gastrointestinal stromal tumor c-KIT oncoprotein: biological and clinical implications. Oncogene 2001;20:5054–8. [PubMed: 11526490]
18. Crouch SP, Kozlowski R, Slater KJ, Fletcher J. The use of ATP bioluminescence as a measure of cell proliferation and cytotoxicity. J Immunol Methods 1993;160:81–8. [PubMed: 7680699]
19. Garcia-Calvo M, Peterson EP, Leiting B, Ruel R, Nicholson DW, Thornberry NA. Inhibition of human caspases by peptide-based and macromolecular inhibitors. J Biol Chem 1998;273:32608–13. [PubMed: 9829999]

20. Karvinen J, Hurskainen P, Gopalakrishnan S, Burns D, Warrior U, Hemmila I. Homogeneous time-resolved fluorescence quenching assay (LANCE) for caspase-3. J Biomol Screen 2002;7:223–31. [PubMed: 12097185]
21. Choi Y, Ta M, Atouf F, Lumelsky N. Adult pancreas generates multipotent stem cells and pancreatic and nonpancreatic progeny. Stem Cells 2004;22:1070–84. [PubMed: 15536197]
22. Duensing A, Medeiros F, McConarty B, et al. Mechanisms of oncogenic KIT signal transduction in primary gastrointestinal stromal tumors (GISTs). Oncogene 2004;23:3999–4006. [PubMed: 15007386]
23. Rubin BP, Singer S, Tsao C, et al. KIT activation is a ubiquitous feature of gastrointestinal stromal tumors. Cancer Res 2001;61:8118–21. [PubMed: 11719439]
24. Ou WB, Zhu MJ, Demetri GD, Fletcher CD, Fletcher JA. Protein kinase C-theta regulates KIT expression and proliferation in gastrointestinal stromal tumors. Oncogene. 2008
25. Hirota S, Isozaki K, Moriyama Y, et al. Gain-of-function mutations of c-kit in human gastrointestinal stromal tumors. Science 1998;279:577–80. [PubMed: 9438854]
26. Dematteo RP, Lewis JJ, Leung D, Mudan SS, Woodruff JM, Brennan MF. Two hundred gastrointestinal stromal tumors: recurrence patterns and prognostic factors for survival. Ann Surg 2000;231:51–8. [PubMed: 10636102]
27. Heinrich MC, Corless CL, Demetri GD, et al. Kinase mutations and imatinib response in patients with metastatic gastrointestinal stromal tumor. J Clin Oncol 2003;21:4342–9. [PubMed: 14645423]
28. Heinrich MC, Corless CL, Blanke CD, et al. Molecular correlates of imatinib resistance in gastrointestinal stromal tumors. J Clin Oncol 2006;24:4764–74. [PubMed: 16954519]
29. Weisberg E, Manley PW, Breitenstein W, et al. Characterization of AMN107, a selective inhibitor of native and mutant Bcr-Abl. Cancer Cell 2005;7:129–41. [PubMed: 15710326]
30. Prenen H, Deroose C, Vermaelen P, et al. Establishment of a mouse gastrointestinal stromal tumour model and evaluation of response to imatinib by small animal positron emission tomography. Anticancer Res 2006;26:1247–52. [PubMed: 16619531]
31. Prenen H, Guetens G, de Boeck G, et al. Cellular uptake of the tyrosine kinase inhibitors imatinib and AMN107 in gastrointestinal stromal tumor cell lines. Pharmacology 2006;77:11–6. [PubMed: 16534250]
32. Heinrich MC, Corless CL, Blanke CD, et al. Molecular Correlates of Imatinib Resistance in Gastrointestinal Stromal Tumors. J Clin Oncol. 2006
33. Wardelmann E, Merkelbach-Bruse S, Pauls K, et al. Polyclonal evolution of multiple secondary KIT mutations in gastrointestinal stromal tumors under treatment with imatinib mesylate. Clin Cancer Res 2006;12:1743–9. [PubMed: 16551858]
34. Bauer S, Duensing A, Demetri GD, Fletcher JA. KIT oncogenic signaling mechanisms in imatinib-resistant gastrointestinal stromal tumor: PI3-kinase/AKT is a crucial survival pathway. Oncogene 2007;26:7560–8. [PubMed: 17546049]
35. Oosterom AT, Dumez H, Desai J, et al. Combination signal transduction inhibition: A phase I/II trial of the oral mTOR-inhibitor everolimus (E, RAD001) and imatinib mesylate (IM) in patients (pts) with gastrointestinal stromal tumor (GIST) refractory to IM. Proc Am Soc Clin Oncol 2004;24:3002.
36. Bauer, S.; Yu, L.; Read, M.; Normant, E.; Demetri, GD.; Fletcher, JA. AACR- NCI-EORTC Molecular targets and cancer therapeutics. Philadelphia: 2005. IPI504, a novel HSP90 inhibitor, causes inhibition and degradation of KIT in imatinibresistant GIST: rationale for therapeutic targeting in GIST; p. C49
37. Demetri GD, George S, Morgan JA, et al. Inhibition of the Heat Shock Protein 90 (Hsp90) chaperone with the novel agent IPI-504 to overcome resistance to tyrosine kinase inhibitors (TKIs) in metastatic GIST: Updated results of a phase I trial. J Clin Oncol 2007;25:10024.
38. Berger SL. The complex language of chromatin regulation during transcription. Nature 2007;447:407–12. [PubMed: 17522673]
39. Marks PA, Richon VM, Miller T, Kelly WK. Histone deacetylase inhibitors. Adv Cancer Res 2004;91:137–68. [PubMed: 15327890]
40. Glozak MA, Seto E. Histone deacetylases and cancer. Oncogene 2007;26:5420–32. [PubMed: 17694083]

41. Song J, Noh JH, Lee JH, et al. Increased expression of histone deacetylase 2 is found in human gastric cancer. APMIS 2005;113:264–8. [PubMed: 15865607]

42. Hrzenjak A, Moinfar F, Kremser ML, et al. Valproate inhibition of histone deacetylase 2 affects differentiation and decreases proliferation of endometrial stromal sarcoma cells. Mol Cancer Ther 2006;5:2203–10. [PubMed: 16985053]

43. Nimmanapalli R, Fuino L, Bali P, et al. Histone deacetylase inhibitor LAQ824 both lowers expression and promotes proteasomal degradation of Bcr-Abl and induces apoptosis of imatinib mesylate-sensitive or -refractory chronic myelogenous leukemia-blast crisis cells. Cancer Res 2003;63:5126–35. [PubMed: 12941844]

44. Nimmanapalli R, Fuino L, Stobaugh C, Richon V, Bhalla K. Cotreatment with the histone deacetylase inhibitor suberoylanilide hydroxamic acid (SAHA) enhances imatinib-induced apoptosis of Bcr-Abl-positive human acute leukemia cells. Blood 2003;101:3236–9. [PubMed: 12446442]

45. Zhang C, Richon V, Ni X, Talpur R, Duvic M. Selective induction of apoptosis by histone deacetylase inhibitor SAHA in cutaneous T-cell lymphoma cells: relevance to mechanism of therapeutic action. J Invest Dermatol 2005;125:1045–52. [PubMed: 16297208]

46. Scroggins BT, Robzyk K, Wang D, et al. An acetylation site in the middle domain of Hsp90 regulates chaperone function. Mol Cell 2007;25:151–9. [PubMed: 17218278]

47. Murphy PJ, Morishima Y, Kovacs JJ, Yao TP, Pratt WB. Regulation of the dynamics of hsp90 action on the glucocorticoid receptor by acetylation/deacetylation of the chaperone. J Biol Chem 2005;280:33792–9. [PubMed: 16087666]

48. Yu C, Dasmahapatra G, Dent P, Grant S. Synergistic interactions between MEK1/2 and histone deacetylase inhibitors in BCR/ABL+ human leukemia cells. Leukemia 2005;19:1579–89. [PubMed: 16015388]

49. Richon VM, Sandhoff TW, Rifkind RA, Marks PA. Histone deacetylase inhibitor selectively induces p21(WAF1) expression and gene-associated histone acetylation. Proceedings of the National Academy of Sciences of the United States of America 2000;97:10014–9. [PubMed: 10954755]

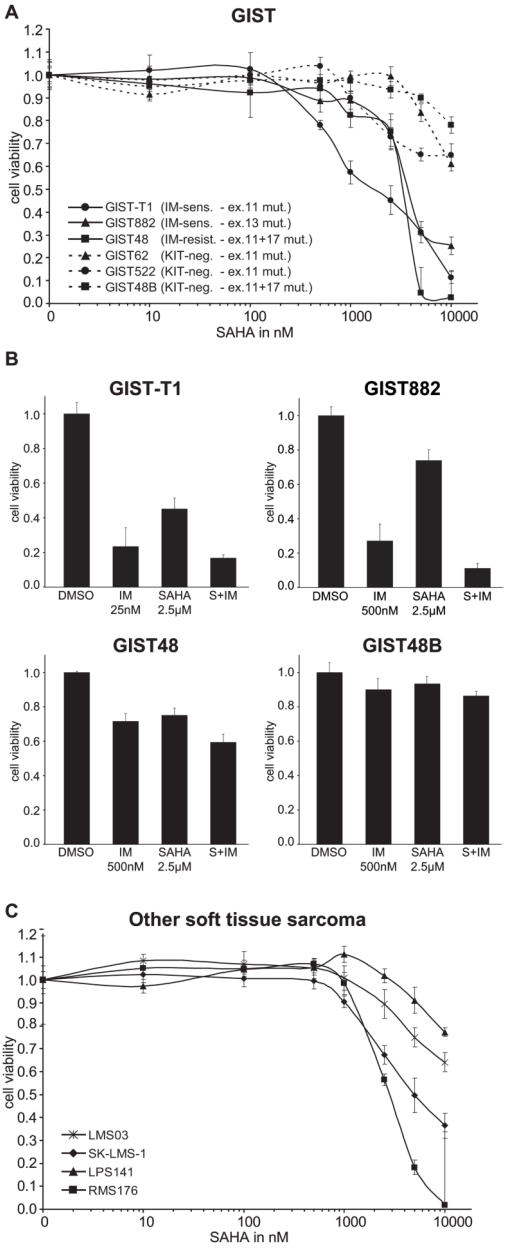

Figure 1.

A: CellTiter-Glo ATP-based viability assays for SAHA in imatinib-sensitive (GIST882, GIST-T1) and imatinib-resistant (GIST48, GIST48B, GIST62, GIST522) cell lines. All cells were treated with the indicated concentrations and assessed after 3 days of treatment, with the data normalized to DMSO-only controls. x = 0 is DMSO-only treated. *Lines*, KIT-positive cell lines; *dotted lines*, KIT-negative cell lines, *points*, mean of quadruplicate cultures; *bars*, SD.

B: Treatment with DMSO, IM or SAHA alone and a combination of SAHA 2.5 μM and IM 500 nM in 4 GIST cell lines.

C: Treatment of other, KIT-negative, IM-resistant soft tissue sarcoma cell lines with SAHA.

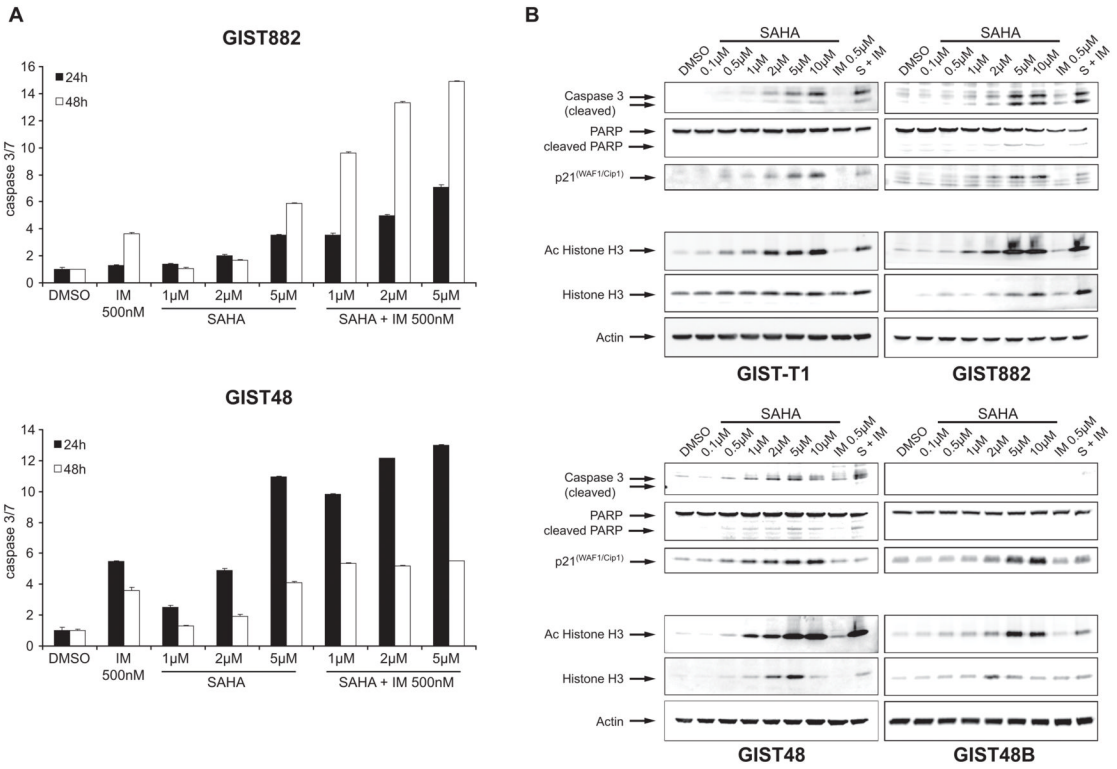

Figure 2.

A: Induction of apoptosis represented by amount of activated caspases 3 and 7 as measured by a luminescence based assay (Caspase-Glo®). Indicated concentrations of SAHA were assayed alone and in combination with IM (500 nM) in KIT-positive GIST after 24h and 48h of incubation. DMSO was vehicle control. *Bars*, mean of quadruplicate cultures with SD represent multitudes of DMSO-only values.

B: Immunoblotting of apoptosis markers (cleaved Caspase 3 and PARP), p21 and acetylation of histone H3, after 18h of treatment with increasing doses of SAHA, IM (500 nM), and a combination of SAHA (2 μM) and IM (500 nM) in IM-sensitive (GIST-T1 and GIST882) and IM-resistant (GIST48 and GIST48B) GIST cell lines. Actin served as control for equal protein loading.

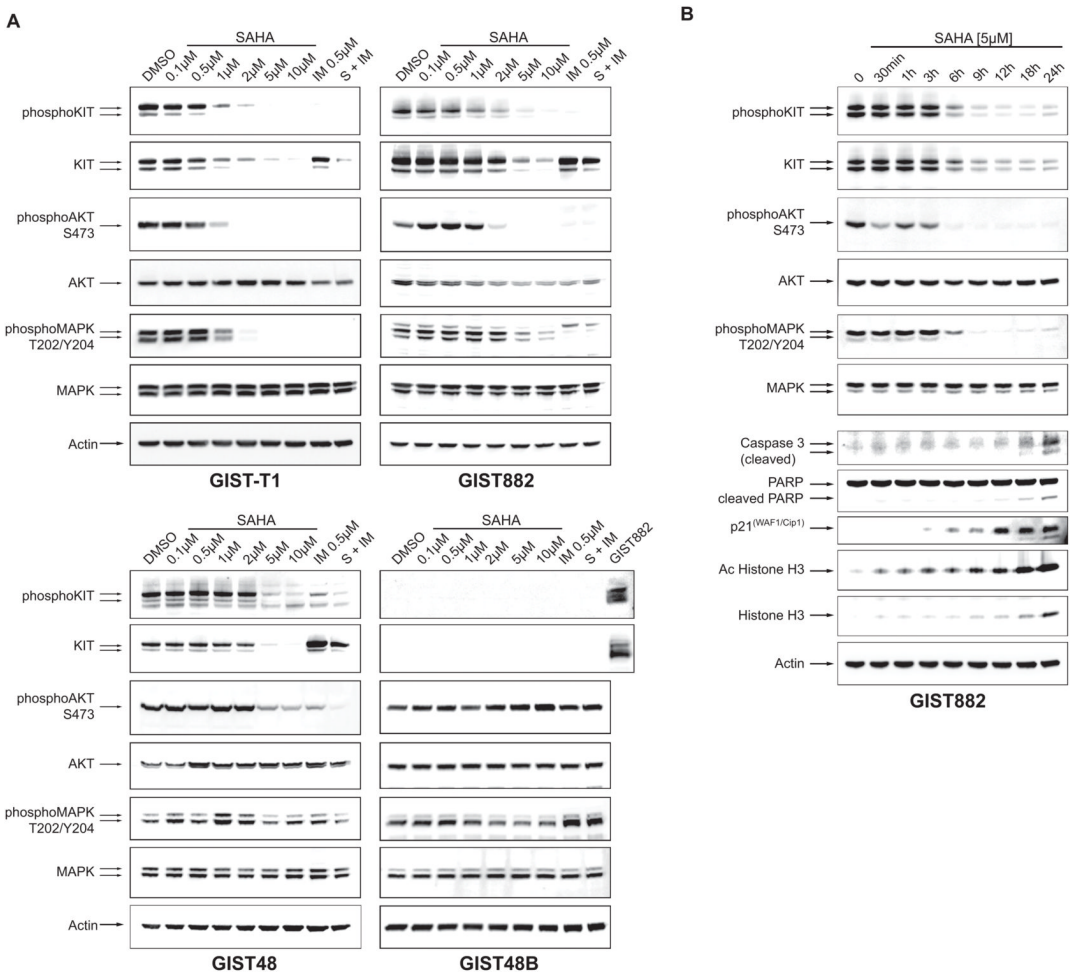

Figure 3.

Western Blot analyses of SAHA effects on KIT and KIT-dependent signaling pathways.

A: Dose-response study after 18h of incubation with increasing doses of SAHA, IM (500 nM), and a combination (S + IM) of SAHA (2 μM) and IM (500 nM).

In KIT-negative GIST48B, untreated GIST882-lysate served as positive control for KIT-staining.

B: Time course study in GIST882. Cells treated for indicated intervals with SAHA 5 μM.

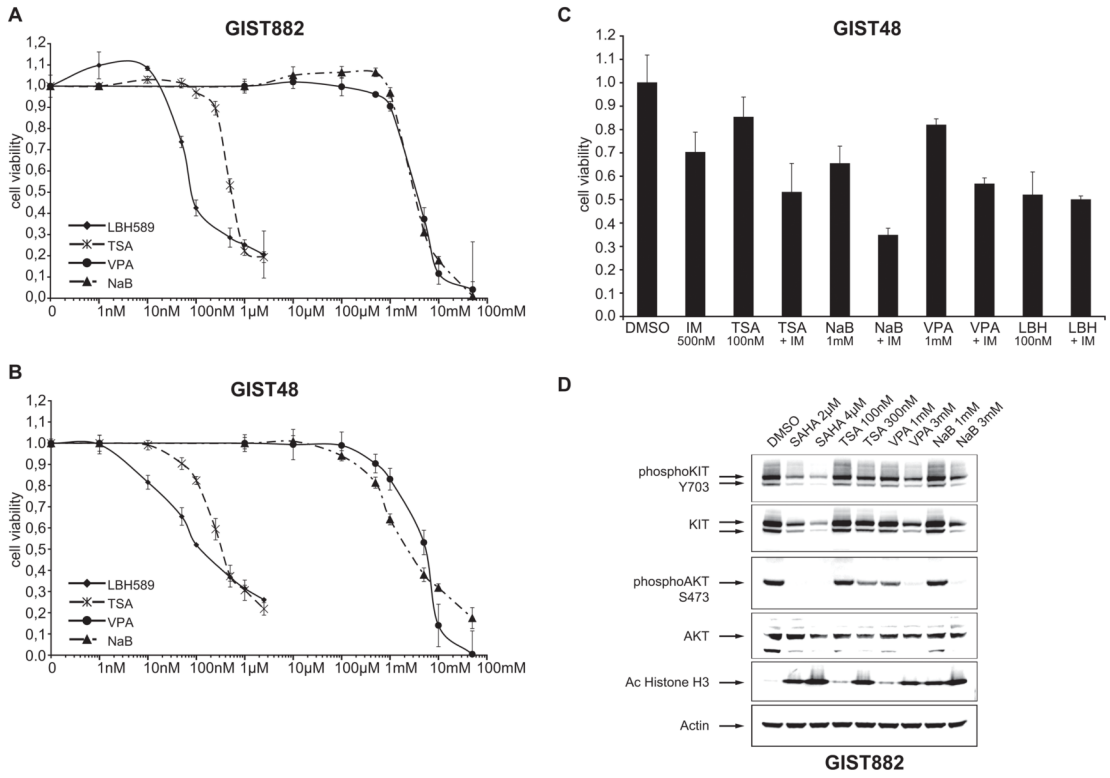

Figure 4.

Effects of various HDACI on KIT-positive GIST.

A, B: Viability studies (72h) for different HDACI in GIST882 and GIST48

C: Combination treatments of HDACI with IM 500 nM in GIST48 after 3 days of treatment

D: Immunoblot studies of different HDACI on oncogenic KIT signaling and Histone acetylation in GIST882.

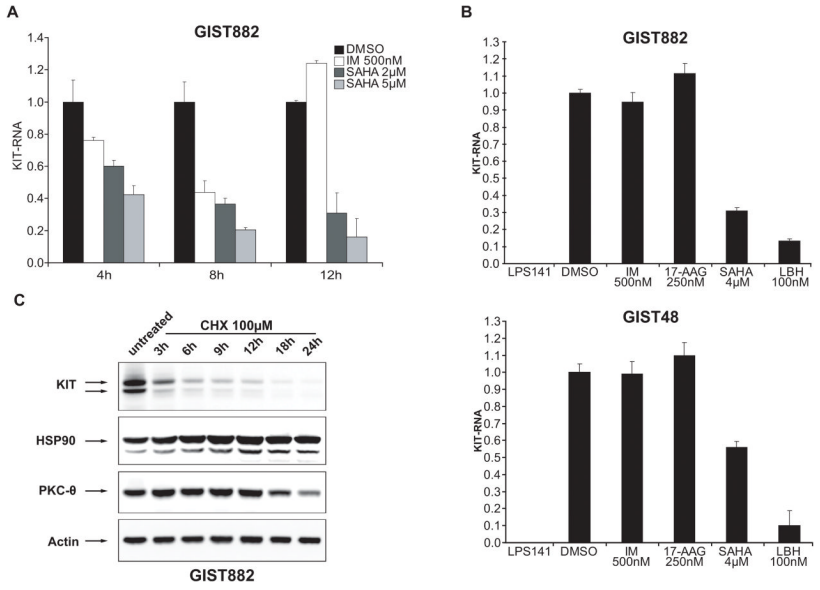

Figure 5.

Effects of different inhibitors on KIT mRNA and Protein levels

A, B: Quantitative Real Time RT-PCR evaluation of *KIT* mRNA in KIT-positive GIST. Time course study (4, 8 and 12 hours of treatment) with IM 500 nM and 2 concentrations of SAHA (2 μM and 5 μM) (A). Comparison of KIT-inhibitor IM, HSP90-inhibitor 17-AAG and HDAC-inhibitors SAHA and LBH589 on KIT-RNA levels after 12h of treatment (B). Values were normalized to the DMSO value for each point in time.

C: Western Blot studies of GIST882 treated with 100 μM cycloheximide (CHX) from 3h to 24h.

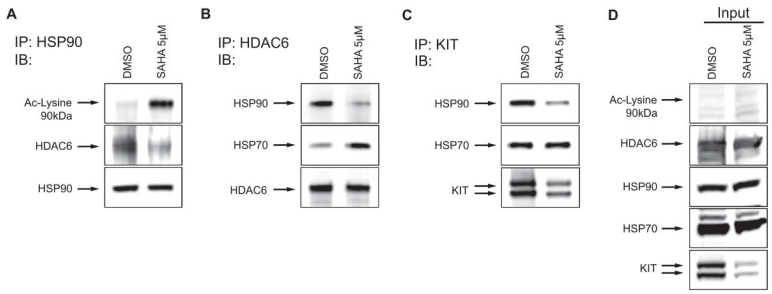

Figure 6.

Immunoprecipitation of HSP90 (A), HDAC6 (B) and KIT (C) from GIST882 cell lysates treated with DMSO and SAHA 5 μM for 12 hours. D: Staining of whole cell lysates (Inputs) for the indicated proteins.